

# High-Spatioresolved Microarchitectural Surface Prepared by Photograft Copolymerization Using Dithiocarbamate: Surface Preparation and Cellular Responses

J. Higashi,<sup>†,‡,§,||</sup> Y. Nakayama,<sup>†,‡</sup> R. E. Marchant,<sup>||</sup> and T. Matsuda<sup>\*,‡</sup>

Department of Bioengineering, National Cardiovascular Center Research Institute, 5-7-1 Fujishiro-dai, Suita, Osaka 565-8565, Japan, School of Medicine and Department of Biomedical Engineering, Case Western Reserve University, Wickenden Building 504, 10900 Euclid Avenue, Cleveland, Ohio 44106-7207

Received August 18, 1998. In Final Form: December 31, 1998

Self-perpetuating photograft copolymerization based on the photochemistry of an iniferter benzyl *N,N*-diethyldithiocarbamate was utilized to design two types of microprocessed surfaces using a custom-designed apparatus operated by an X–Y step motor. Cellular adhesion and growth responses were studied on (1) a surface upon which five different water soluble polymer regions were photografted with micron order precision and (2) three different gradient surfaces with unidirectionally varying thicknesses of a water soluble graft polymer layer. A striped micropatterned surface (width of each region 500  $\mu\text{m}$ ) was prepared by sequential photoirradiation through a photomask with a stripe window on a selected region of a poly-(styrene-*co*-vinylbenzyl *N,N*-diethyldithiocarbamate)-coated PET film immersed in an aqueous solution of vinyl monomer. The sample stage was moved in a stepwise manner for each change of monomer solution. The monomers studied were *N,N*-dimethylacrylamide (DMAAm), 2-hydroxyethyl methacrylate (HEMA), *N*-[3-(dimethylamino)propyl]acrylamide methiodide (DMAPAAMeI), methacrylic acid sodium salt (MANa), and 3-sulfopropyl methacrylate potassium salt (SMAK). Surface wettability, X-ray photoelectron spectroscopic analyses, and light microscopic visualization by dye staining revealed that five stripe regions, each of which was grafted with a different polymer, were prepared side by side. Seeding and culture of endothelial cells (ECs) on the micropatterned surfaces yielded markedly reduced adhesion on polyDMAAm and polyHEMA. PolyDMAPAAMeI and polyMANa regions promoted cell adhesion and growth, whereas enhanced adhesion was initially observed but then became markedly reduced over time on polySMAK. Atomic force microscopic (AFM) observation showed that photoirradiation through a photomask in the presence of a monomer solution (DMAAm, DMAPAAMeI, and MANa) under continuous sample movement yielded a graft-polymer-layer thickness gradient surface. EC adhesion and proliferation gradually decreased with increasing graft layer thickness on the polyDMAPAAMeI and polyMANa surfaces. In contrast, cell adhesion on the polyDMAAm-grafted surface ceased abruptly above a certain graft thickness. This study shows that, using this photograft copolymerization method, both regional and chemical specific surface modification on the micron level has been achieved, representing a significant advance in the microprocessing of biomedical devices.

## Introduction

Cellular behaviors such as adhesion and proliferation on surfaces are critical factors determining surfaces' blood and tissue compatibility.<sup>1–4</sup> Nonionic hydrated graft surfaces are generally resistant to both protein adsorption and cellular adhesion, whereas polar, hydrophobic, and ionic surfaces often promote cellular adhesion and proliferation. Most previous studies examining cellular behavior on material surfaces have been conducted on individual substrates. This approach can be both time-consuming and labor-intensive, increasing the likelihood of sample to sample variability during cell culture experi-

ments. Thus, there is considerable impetus to develop methods to produce regionally specific, multifunctionalized surfaces where the effect of selected physicochemical properties and chemical compositions or species on cell behavior can be studied in one experiment on one surface. To this end, efforts have been directed at developing several types of gradient surfaces, where surface functional group density and graft chain density are unidirectionally varied for the purpose of studying both protein adsorption and cell adhesion as a function of these surface parameters.<sup>5–12</sup>

Recently, we developed a photochemical surface modification technique that enables surface polymerization with micrometer order regional precision using the photochemistry of benzyl *N,N*-diethyldithiocarbamate, an

\* Corresponding Author. Telephone: +81-6-6833-5012. Fax: +81-6-6872-7485.

<sup>†</sup> Co-first authors.

<sup>‡</sup> National Cardiovascular Center Research Institute.

<sup>§</sup> School of Medicine, Case Western Reserve University.

<sup>||</sup> Department of Biomedical Engineering, Case Western Reserve University.

(1) Szycher, M. *Biocompatible Polymers, Metals and Composites*; Technomic Publ., Co., Inc.: Lancaster, 1983.

(2) Park, J. B. *Biomaterials Science and Bioengineering*; Plenum Press: New York and London, 1984.

(3) Andrade, J. D. In *Surface and Interfacial Aspects of Biomedical Polymers*; Andrade, J. D., Ed.; Plenum Press: New York, 1985; Vol. 1, p 1.

(4) Curtis, A. S. G. *Cell Adhesion. The Cell Surface; Its Molecular Role in Morphogenesis*; London/Logos/Academic Press: 1967.

(5) Hlady, V.; Golander, C.; Andrade, J. D. *Colloids Surf.* **1987**, *25*, 185.

(6) Lin, Y. S.; Hlady, V.; Janatova, J. *Biomaterials* **1992**, *13*, 497.

(7) Elwing, H.; Welin, S.; Askendal, A.; Nilsson, U.; Lundstrom, I. *J. Colloid Interface Sci.* **1987**, *119*, 203.

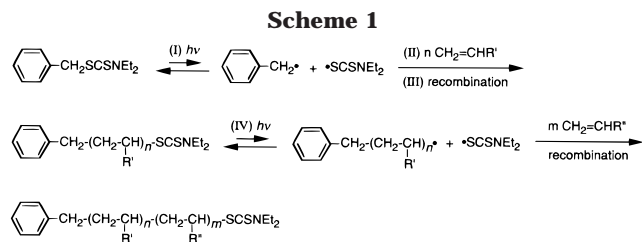
(8) Elwing, H.; Askendal, A.; Lundstrom, I. *J. Biomed. Mater. Res.* **1987**, *21*, 1023.

(9) Golander, C. G.; Pitt, W. G. *Biomaterials* **1990**, *11*, 32.

(10) Lee, J. H.; Lee, H. B. *J. Biomater. Sci., Polym. Ed.* **1993**, *4*, 467.

(11) Lee, J. H.; Khang, G.; Lae, J. W.; Lae, H. B. *J. Biomed. Mater. Res.* **1998**, *40*, 180.

(12) Ueda, T. Y.; Matsuda, T. *Langmuir* **1995**, *11*, 4135.



“iniferter”, pioneered by Otsu et al.<sup>13–17</sup> as illustrated in Scheme 1. The benzyl radical produced by photolysis of the iniferter (reaction I in Scheme 1) can react with a given vinyl monomer to initiate a free radical polymerization reaction (reaction II). A dithiocarbamate free radical hardly reacts with a vinyl monomer but favorably recombines with a growing polymer chain radical to generate a dithiocarbamate end (dormant propagation end) (reaction III) that again regenerates a radical pair upon photolysis (reaction IV). Our previous study showed that the advantages of this surface photopolymerization technique are (1) regional control, (2) two-dimensional precision, and (3) self-perpetuating polymerization, enabling chain length control. Using this approach, we prepared a two-dimensional micropatterned tissue of endothelial cells by utilizing the inherent differences in cell adhesiveness of different micropatterned photografted regions. In addition, a single gradient surface where the graft polymer chain length was unidirectionally varied was prepared by changing the photointensity using a gradient neutral-density filter.<sup>18</sup> This study suggests that the *N,N*-diethyldithiocarbamate photochemistry can be an effective tool to control surface characteristics and therefore cellular responses on biomedical devices.

The objectives of this study were to extend the previous work by demonstrating the ability to prepare two types of microprocessed surfaces [(1) a micropatterned surface with an unprecedented five different photograft copolymerized regions and (2) three different photograft-copolymer-layer-thickness gradient surfaces] and then to examine endothelial cell adhesion and proliferation on these surfaces. The ability to precisely multifunctionalize films on one physical sample with regional specificity enabled the simultaneous evaluation of cellular response on the grafted films, thus efficiently reducing sample-to-sample variability. However, the greater implications of this technique rest in the possibility to precisely control the surface chemistry to optimize cellular responses on a micron order level. In addition, the graft-polymer-layer-thickness surfaces allowed a controlled examination of the effect of polymer chain length on cellular response within one physical sample. With these novel surfaces, initial studies involving the simultaneous characterization of cellular responses in multiple surface microenvironments have been completed.

### Materials and Methods

**Materials.** Styrene (ST) was purchased from Ohken Co., Ltd. (Tokyo, Japan). *N*-[3-(Dimethylamino)propyl]acrylamide (DMA-PAAm) was obtained from Kohjin Co., Ltd. (Tokyo, Japan). The nitrogen methiodide of DMA-PAAm (DMA-PAAmMeI) was pre-

(13) Otsu, T.; Yoshida, M. *Makromol. Chem., Rapid Commun.* **1982**, 3, 127.

(14) Otsu, T.; Yoshida, M.; Tazaki, T. *Makromol. Chem., Rapid Commun.* **1982**, 3, 133.

(15) Otsu, T.; Yoshida, M. *Polym. Bull* (Berlin) **1982**, 7, 197.

(16) Otsu, T.; Matsunaga, T.; Doi, T.; Matsumoto, A. *Eur. Polym. J.* **1995**, 31, 67.

(17) Otsu, T.; Matsumoto, A. *Adv. Polym. Sci.* **1998**, 136, 75.

(18) Nakayama, Y.; Matsuda, T. *Macromolecules* **1996**, 29, 8622.

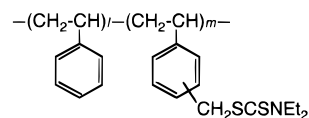


**Figure 1.** Chemical structure of the photoreactive copolymer poly(styrene-*co*-vinylbenzyl *N,N*-diethyldithiocarbamate); *l*:*m* = 51:49.

pared by addition of methyl iodide to an ethanol solution of DMA-PAAm.<sup>19</sup> 3-Sulfopropyl methacrylate potassium salt was obtained from Aldrich Chemical Co., Inc. (Milwaukee, WI). *N,N*-Dimethylacrylamide (DMAAm), 2-hydroxyethyl methacrylate (HEMA), methacrylic acid sodium salt (MANa), solvents, and other reagents, all of which are of special reagent grade, were obtained from Wako Pure Chem. Ind., Ltd. (Osaka, Japan) and used after standard purification (2,2'-Azobis(isobutyronitrile) (AIBN) was recrystallized twice from methanol. Poly(ethylene terephthalate) (PET) circular film (diameter, 14 mm; thickness, 200  $\mu$ m) was obtained from Wako.

**Preparation of Photoreactive Copolymer.** Details of the preparation of the photoreactive copolymer (Figure 1) were described in our previous paper.<sup>18</sup> Briefly, ST (0.83 g, 8.0 mmol) and vinylbenzyl *N,N*-diethyldithiocarbamate (*m* and *p* mixture, 2.12 g, 8.0 mmol) prepared from vinylbenzyl chloride and sodium *N,N*-diethyldithiocarbamate were copolymerized in the presence of AIBN ([monomer]/[initiator] = 100, molar ratio) in *N,N*-dimethylformamide (DMF) (30 mL) in the dark for 10 h at 60 °C. The yield was 0.47 g (15.9%). The molecular weight of the polymer, estimated by gel permeation chromatography (GPC) analysis, was  $M_n$  = 37 000 (PST standard; eluent  $\text{CHCl}_3$ ). The content of photoreactive moiety in the copolymer, determined by <sup>1</sup>H NMR spectroscopy, was 49.3 mol %.

**Surface Graft Copolymerization.** The photoreactive copolymer in toluene solution (2 wt %) was cast on one side of the PET films. Five different vinyl monomer-containing aqueous solutions (concentration of monomer: 0.5 mol/dm<sup>3</sup> for DMAAm, DMA-PAAm, HEMA, and SMA; 1.0 mol/dm<sup>3</sup> for MANa) were prepared, and a stream of dry nitrogen gas was bubbled through each solution. A custom-designed reaction vessel, in which one coated PET film was placed, was filled with the appropriate vinyl monomer solution and covered with a sapphire plate. Each sample was then UV-irradiated from a locus of approximately 30 mm with light from an ultrahigh-pressure mercury-vapor lamp (250 W, SPOT CURE250, Ushio, Tokyo, Japan) through a quartz optical fiber (diameter, 5 mm; length, 1 m) for 10 min. The light intensity, measured with a photometer (UVR-1, Topcon, Tokyo, Japan), was 0.5 mW/cm<sup>2</sup>. The temperature of the polymerized samples was maintained at 20–25 °C. The treated films were thoroughly rinsed with distilled water, methanol, and ethanol to remove unreacted monomer and polymer in solution and dried in air.

**Preparation of Micropatterned Surface.** The photoreactive copolymer-coated PET film was placed on an X–Y step motor-controlled stage (Mini-40XY, Sigma Koki Co., Ltd., Saitama, Japan), and a reaction vessel installed with a photomask with a slit width of 500  $\mu$ m was fitted tightly on the film (Koyo Co., Ltd., Tokyo, Japan). The reaction vessel was filled with the first monomer solution and covered with a sapphire plate. The film was irradiated with UV light through the photomask for 10 min, as described above. The film was then rinsed with water and alcohols and dried in air. The stage was then moved by 500  $\mu$ m unidirectionally. The treated film was placed again on the stage and subsequently irradiated in the presence of the second monomer solution in the same manner as described above. A micropatterned surface with five different photografted regions was prepared by repeatedly moving the stage and applying UV irradiation in the presence of the appropriate monomer solution. The grafted polymers were stained with a dilute hydrochloric acid solution of malachite green carbinol base (1.0 w/v %, polyMANa) and with a dilute aqueous solution of rose bengal (Acid Red 94, C.I. 45440) (1.0 w/v %, for polyDMA-PAAmMeI) for visualization under a light microscope with a Nikon Optiphot system (Tokyo, Japan).

(19) Snyder, H. R.; Eliel, E. L. *J. Am. Chem. Soc.* **1948**, 70, 1703.

**Table 1. Chemical Compositions and Water Contact Angles of Photograft-Copolymerized Surfaces**

surface	elemental ratio <sup>a</sup>			contact angle <sup>c</sup> (deg)	
	N/C	O/C	other	advancing	receding
PET sheet (substrate)	0 (0)	0.35 (0.40)	<i>b</i>	63.2 ± 2.6	60.2 ± 2.1
photoreactive copolymer-coated	0.04 (0.05)	0.05 (0)	0.07 (0.09; S/C)	83.4 ± 1.3	78.2 ± 2.3
DMAAm graft-copolymerized	0.20 (0.20)	0.18 (0.20)	<i>b</i>	31.6 ± 3.6	11.8 ± 3.5
HEMA graft-copolymerized	0.02 (0)	0.41 (0.50)	<i>b</i>	44.5 ± 2.5	13.3 ± 3.3
DMAAmMeI graft-copolymerized	0.14 (0.22)	0.13 (0.11)	1.2 (1.0; N/I)	29.2 ± 2.8	<5
MANa graft-copolymerized	0.01 (0)	0.49 (0.50)	0.13 (0.25; Na/C)	25.3 ± 3.3	<5
SMAK graft-copolymerized	0.03 (0)	0.53 (0.71)	0.25 (0.14; K/C)	14.8 ± 2.2	<5
			0.12 (0.14; S/C)		

<sup>a</sup> Values as obtained by XPS measurements. Parentheses show theoretical values. <sup>b</sup> Not measured. <sup>c</sup> Measured by the sessile drop method.

**Preparation of Graft-Polymer-Layer-Thickness Gradient Surface.** The photoreactive copolymer-coated PET films were fixed on the X–Y step motor-controlled stage and were covered with a stripe pattern photomask (width of lines: 450 μm). The films were UV-irradiated in the presence of an aqueous monomer solution (DMAAm, DMAAmMeI, and MANa) in the same manner as described above while continuously moving the stage unidirectionally at a rate of 2.2 μm/s for 15 min.

**Surface Characterization.** The chemical composition of the outermost surface layer was determined by X-ray photoelectron spectroscopy (ESCA 750, Shimadzu, Kyoto, Japan) using a magnesium anode (Mg K $\alpha$  radiation) connected to a data processor ESCAPAC-760 at room temperature and  $2 \times 10^{-7}$  Torr (8 kV, 20 mA) at a takeoff angle of 90°, where the takeoff angle is defined as the angle between the sample surface and the electron optics of the energy analyzer.

The wettability of treated surfaces was evaluated by water contact angle measurements using the sessile drop technique with a contact angle meter (CA-D, Kyowa Kaimenkagaku Co., Ltd., Tokyo, Japan).

Observation of the surface topography of each graft-copolymerized film and its thickness was performed by atomic force microscopy (AFM, NanoScope III, Digital Instruments, Inc., Santa Barbara, CA) using a Si<sub>3</sub>N<sub>4</sub> cantilever with a spring constant of 0.12 N/m (reported by Digital Instruments, Inc.). The cantilever was V-shaped and 200 μm long, operated at –1.0 V at a scanning rate of 1.0 Hz. AFM images (400 pixels × 400 pixels) were obtained using the “height mode”, which kept the force constant, and visualized using the “surface mode”. All AFM data manipulations and image processing were carried out with Digital Instruments software.

**Assay of Cellular Responses on Microprocessed Surfaces.** Endothelial cells (ECs), harvested from bovine thoracic aorta by collagenase digestion, were cultured in Dulbecco's modified Eagle's medium (DMEM; Flow Laboratories, McLean, VA) supplemented with 15% fetal bovine serum (HyClone Laboratories, Inc., Logan, UT), a mixture of penicillin and streptomycin (50 mg/L, ICN Biomedicals Inc., Aurora, OH), and amphotericin B (2.5 mg/L, ICN). ECs between the 14th and 16th passages were used. ECs were seeded at a density of  $3 \times 10^4$  cells/well and at 37 °C in a water-saturated 5% CO<sub>2</sub>/95% air atmosphere up to 3 days. The culture medium was replaced every day. Selected samples ( $n = 1$ ) were observed by phase-contrast microscopy (Nikon Diaphoto, Tokyo, Japan) and photographed in 1–3 fields per functionalized region with a Nikon camera (HFX) using Polaroid 667 film (Polaroid, Cambridge, MA), and the number of adherent ECs/unit area was counted.

## Results

Since surface photograft copolymerization initiated by the dithiocarbamate group proceeds via living-like radical polymerization only at UV-irradiated regions and during photoirradiation,<sup>13–18</sup> a two-dimensional micropattern regionally grafted with different polymers or regionally grafted with different chain lengths can be processed using both a photomask and precise motor-controlled sample movement. First, the characterization of graft-copolymerized surfaces was carried out. Then, the preparation of microprocessed surfaces and cellular responses was described.

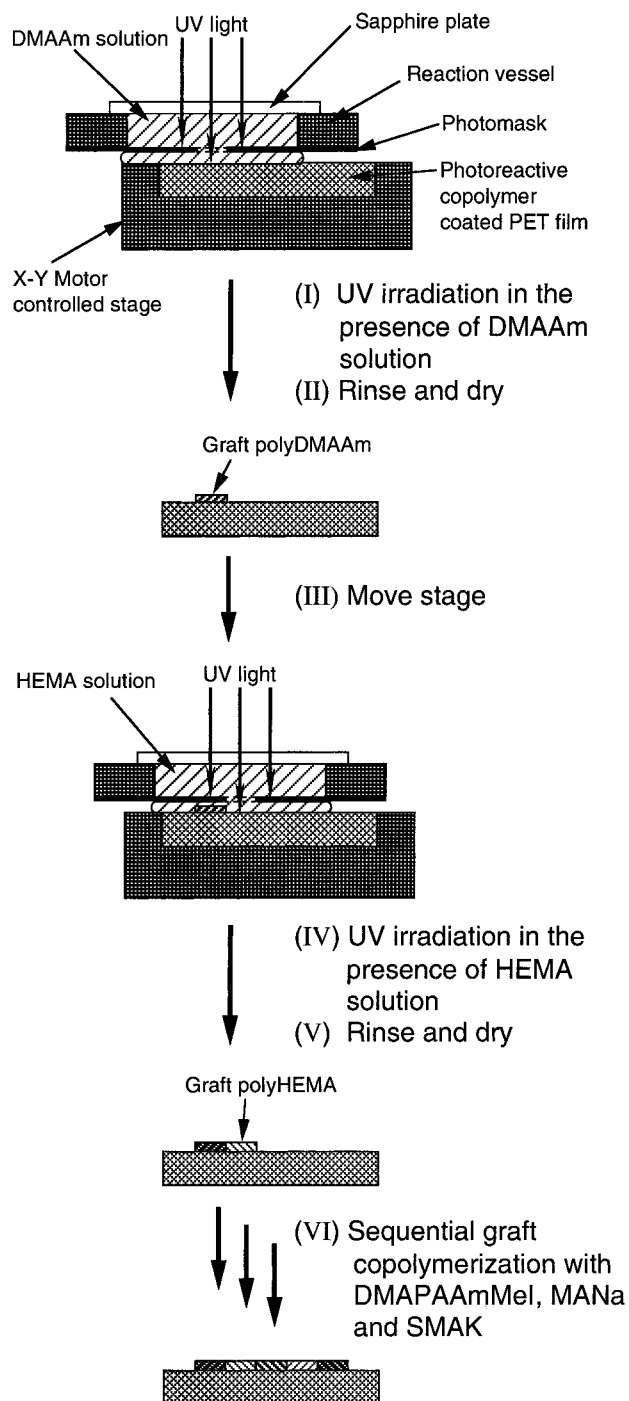


**Figure 2.** Schematic diagram of the preparation of a regionally specific micropatterned surface with an unprecedented five different photograft-copolymerized regions using the combination of a photomask and an X–Y step motor-controlled stage.

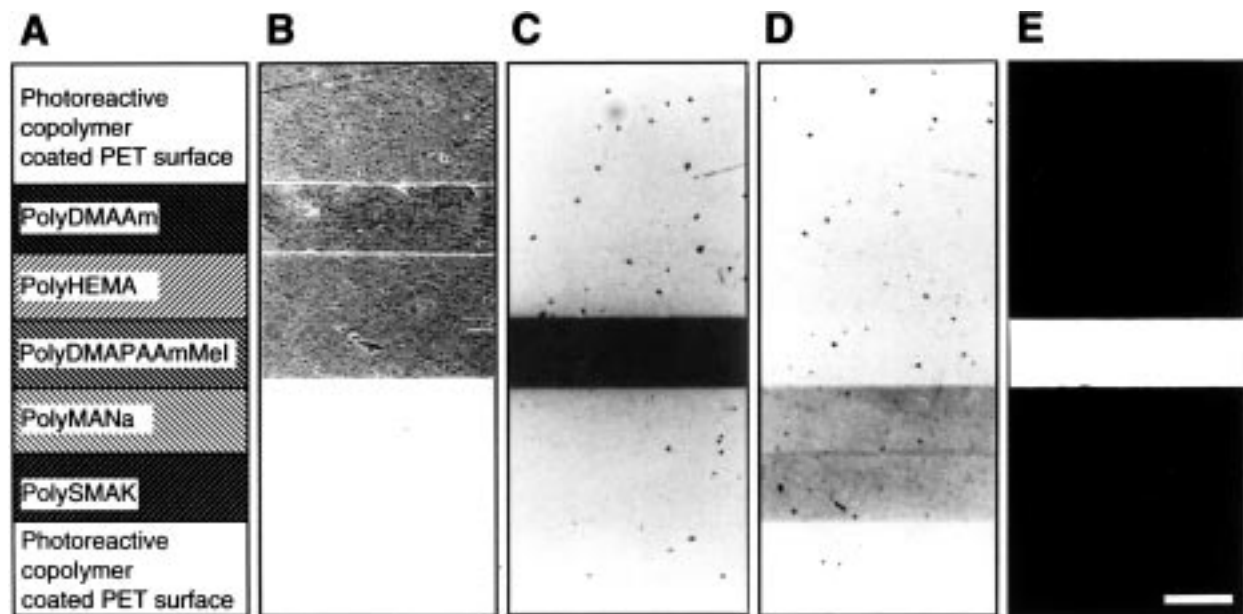


**Figure 3.** Schematic diagram of a regionally specific photograft-copolymerized micropatterned surface shown at a magnification corresponding with the microscopic image (A). Phase-contrast micrograph ( $\times 200$ ) of a polyDMAAm-graft-copolymerized micropatterned surface (B), and micrographs ( $\times 200$ ) of polyDMAPAAMeI- (C) and polyHEMA- and polySMAK- (D) graft-copolymerized micropatterned surfaces and the photomask used in this experiment (E). The polyDMAPAAMeI-grafted region was stained with rose bengal dye (C) while the polyMANa- and polySMAK-grafted regions were stained with malachite green carbinol base (D). Scale bar:  $500 \mu\text{m}$ .

**Surface Photograft Copolymerization and XPS Analysis.** Surface photograft copolymerization was carried out according to our previous method.<sup>18</sup> Briefly, PET films, coated with poly(ST-*co*-vinylbenzyl *N,N*-diethylthiocarbamate) (copolymer composition, 51:49 by molar ratio) (Figure 1) were UV-irradiated in a vinyl monomer-containing aqueous solution that was bubbled with dry nitrogen gas prior to UV irradiation. The vinyl monomers used were *N,N*-dimethylacrylamide (DMAAm), 2-hydroxyethyl methacrylate (HEMA), *N*-[3-(Dimethylamino)propyl]acrylamide methiodide (DMAPAAMeI), methacrylic acid sodium acid (MANa), and 3-sulfoethyl methacrylate potassium salt (SMAK). On the photoreactive copolymer-coated PET film, the N/C, O/C, and S/C elemental ratios, determined from the peak areas of the  $C_{1s}$ ,  $N_{1s}$ ,  $O_{1s}$ , and  $S_{2p}$  signals in XPS spectra, were 0.04 (theoretical value: 0.05), 0.05 (theoretical value: 0), and 0.07 (theoretical value: 0.09), respectively (Table 1). This indicates that the dithiocarbamate groups were distributed in the surface region of the photoreactive copolymer coated on PET films.

When the photoreactive copolymer-coated PET films were UV-irradiated in the presence of each vinyl monomer, significant XPS spectral changes were noted. UV irradiation in the presence of DMAAm and DMAPAAMeI aqueous solutions resulted in the increases in intensity ratios of both nitrogen and oxygen peaks relative to carbon peaks: for DMAAm, N/C = 0.20 (theoretical value: 0.20) and O/C = 0.18 (theoretical value: 0.20); and for DMAPAAMeI, N/C = 0.14 (theoretical value: 0.22) and O/C = 0.13 (theoretical value: 0.11) (Table 1). In addition, the aromatic satellite peak from the photoreactive copolymer had completely disappeared. For DMAPAAMeI, the iodine signal was newly observed. The N/I elemental ratio after treatment was 1.2 (theoretical value: 1.0). On the other hand, UV irradiation in the presence of HEMA, MANa, and SMAK aqueous solutions resulted in an increased O/C elemental ratio: for HEMA, 0.41 (theoretical value: 0.50), for MANa, 0.49 (theoretical value: 0.50), and for SMAK, 0.53 (theoretical value: 0.71). In addition,

irradiation in the presence of MANa- or SMAK- containing solution resulted in appreciation of the sodium signal or the potassium and sulfur signals. For MANa, the Na/C elemental ratio after treatment was 0.13 (theoretical value: 0.25), and for SMAK, the K/C and S/C elemental ratios were 0.25 (theoretical value: 0.14) and 0.12 (theoretical value: 0.14), respectively. Little XPS spectral change was observed after extensive washing with water and alcohols. These results indicate that polyDMAAm, polyDMAPAAMeI, polyHEMA, polyMANa, and polySMAK fully covered the surfaces.

Contact angle measurements showed that, upon UV irradiation in the presence of all monomer solutions, all the photoreactive copolymer-coated surfaces became highly wettable (Table 1). The receding water contact angle was approximately  $80^\circ$  for the photoreactive copolymer surface and less than about  $15^\circ$  for the irradiated surfaces irrespective of the type of monomer, indicating that hydrophilic surfaces were created on the nongrafted hydrophobic polymer surface. These XPS and wettability data lead to the conclusion that photograft copolymerizations with these five monomers proceed under these experimental conditions. This allows us to employ this photograft copolymerization technique and conditions for preparation of a microprocessed surface, as described below.

**Micropatterned Surface and Regionally Differentiated Cellular Responses.** *Preparation of Micropatterned Surface.* Figure 2 shows a schematic diagram of the preparation procedure for the regionally micropatterned surface. First, a metal photomask with a slit width of  $500 \mu\text{m}$  was fitted tightly on the photoreactive copolymer-coated PET film that was placed on the top of an X-Y step motor-controlled stage. The reaction vessel into which the photomask was placed was filled with DMAAm aqueous solution. The PET film was then UV-irradiated through a sapphire plate and the photomask (step I in Figure 2), and thoroughly rinsed with deionized water, methanol, and ethanol and dried in air at room temperature (step II in Figure 2). Phase-contrast micro-

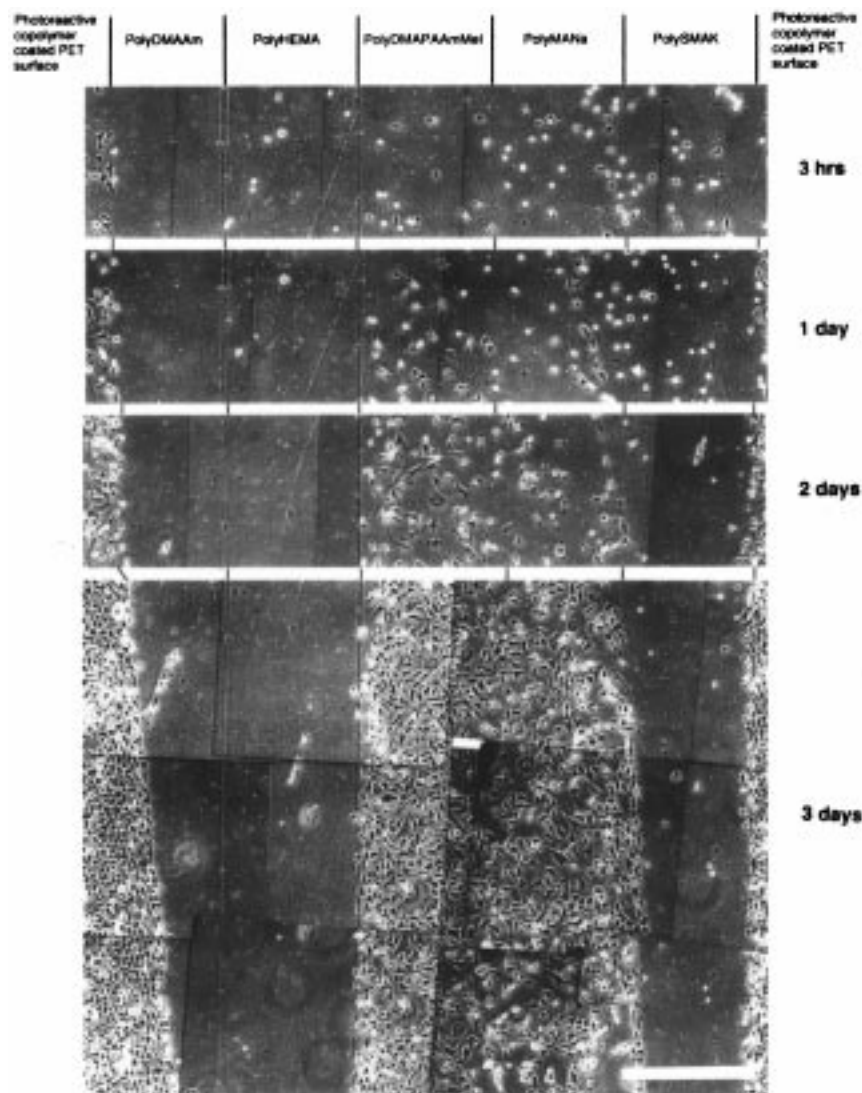


**Figure 4.** Phase-contrast micrographs ( $\times 200$ ) of bovine ECs' adhesion and growth responses on regionally specific photograft-copolymerized micropatterned surfaces over a 3-day incubation. Scale bar:  $200 \mu\text{m}$ .

scopic observation clearly showed the formation of a straight line only at the irradiated region (Figure 3B). The observed width of the line was approximately  $500 \mu\text{m}$ , which was the same as the slit width of the photomask used (Figure 3E). When the irradiated surface was immersed in water, only the line region irradiated in the presence of DMAAm was wetted, indicating that the surface graft copolymerization occurred in a specific manner, resulting in the formation of a grafted hydrophilic polymer domain on the nongrafted hydrophobic photoreactive copolymer-coated surface.

Next, the X–Y step motor-controlled stage was moved by  $500 \mu\text{m}$  unidirectionally (step III in Figure 2). The PET film previously graft-copolymerized with DMAAm was placed again on the stage and subsequently UV-irradiated in the presence of an aqueous solution of the second monomer HEMA (step IV in Figure 2) and then rinsed and dried in the same manner as described above (step V in Figure 2). The operations of moving the stage and further UV irradiation in the presence of aqueous solutions of the other three monomers (DMAPAAMeI, MANa, and SMAK) were repeated three times (step VI in Figure 2). When the thus-treated surface was immersed in an aqueous solution of rose bengal, a dye for positively charged ions, only the third monomer graft-copolymerized region was stained red (Figure 3C). The width of the line was

approximately  $500 \mu\text{m}$ . This indicates that the quaternized aminated monomer DMAPAAMeI was graft-copolymerized in the third line region. As shown in Figure 3D, staining with a dilute HCl solution of malachite green carbinol base, a dye for negatively charged ions, resulted in the formation of a wide line region in green, whose width was approximately  $1000 \mu\text{m}$ , indicating that the anionic carboxylated and sulfonated monomers MANa and SMAK were graft-copolymerized in the fourth and fifth line regions. Thus, DMAAm, HEMA, DMAPAAMeI, MANa, and SMAK were graft-copolymerized in a stepwise manner to form a micropatterned surface composed of five consecutive graft-polymerized regions.

**Cellular Response on Micropatterned Surface.** Bovine ECs were used to examine cellular adhesion and proliferation responses on the micropatterned surface. Figure 4 shows a montage of photomicrographs of daily EC adhesion up to 3 days of incubation on the micropatterned surface, and Figure 5 shows the number of ECs per unit area ( $0.25 \text{ mm}^2$ ) adhering to each region of the micropatterned surface. At 3 h of incubation, the most adherent surface was the photoreactive copolymer-coated PET surface, followed by three ionic monomer-graft-copolymerized surfaces (polyDMAAm, polyMANa, and polySMAK). The least adherent surface was the two nonionic monomer-graft-copolymerized surfaces (polyD-

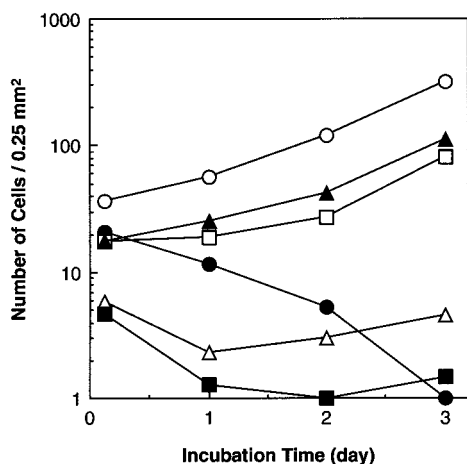


**Figure 5.** Number of bovine ECs that adhered on the nongrafted photoreactive copolymer region (○) and the regions photograft-copolymerized with DMAAm (■), HEMA (△), DMA-PAAmMeI (▲), MANa (□), and SMAK (●) of micropatterned surfaces over a 3-day incubation.

MAAm and polyHEMA). Little sign of proliferation activity was noted for these nonionic surfaces even after periods of culture. Proliferation occurred well on DMAPAAmMeI- and MANa-graft-copolymerized surfaces, whereas the number of adherent cells markedly decreased with incubation time on the SMAK-graft-copolymerized surface. At 3 days incubation, ECs were confluent and exhibited their characteristic cobblestone morphology at both ends of the montage (the photoreactive copolymer-coated PET surface). Markedly reduced cell adhesion was observed for polyDMAAm- and polyHEMA-grafted regions. Few adhered cells were circular in shape. In contrast, ECs on polyDMAPAAM- and polyMANa-grafted regions were highly elongated and subconfluent. Few circular adherent cells were observed on the polySMAK-grafted region.

**Graft-Thickness Gradient Surface and Cellular Responses.** *Preparation of Graft-Thickness Gradient Surface.* Graft-thickness gradient surfaces were prepared by unidirectional continuous control of time of irradiation on a selected region of the photoreactive copolymer-coated PET film (Figure 6). To control the irradiation time, two types of metal photomasks with a line window were used: one (line width: 3 mm) was set at the bottom of a reaction vessel, and the other (line width: 450  $\mu\text{m}$ ) was tightly fixed on the photoreactive copolymer-coated PET film placed on the X–Y step motor-controlled stage. DMAAm, DMAPAAmMeI, and MANa were used as monomers. The reaction vessel was filled with an aqueous solution of the appropriate monomer. The whole assembly was UV-irradiated in the same manner as described above while continuously moving the stage unidirectionally at a rate of 2.2  $\mu\text{m}/\text{s}$  for 15 min (total moving distance: 1.98 mm) (step I in Figure 6). The film was thoroughly rinsed with deionized water and alcohols and dried (step II in Figure 6).

Topographic images of the treated surface were recorded using an atomic force microscope and were acquired at positions with different distances from the starting position of photoirradiation and crossing transversely from an adjacent nonirradiated region. Figure 7 shows the configuration for sampling (Figure 7: 1), AFM images (Figure 7: 2A and 2B), and cross-sectional traces at different positions (Figure 7: 3). The nonirradiated surface (position a in Figure 7: 1) was relatively flat (the surface roughness was estimated to be approximately 50 nm (Figure 7: 3)). On the other hand, the graft-copolymerized layer was uniformly formed on the irradiated surface,

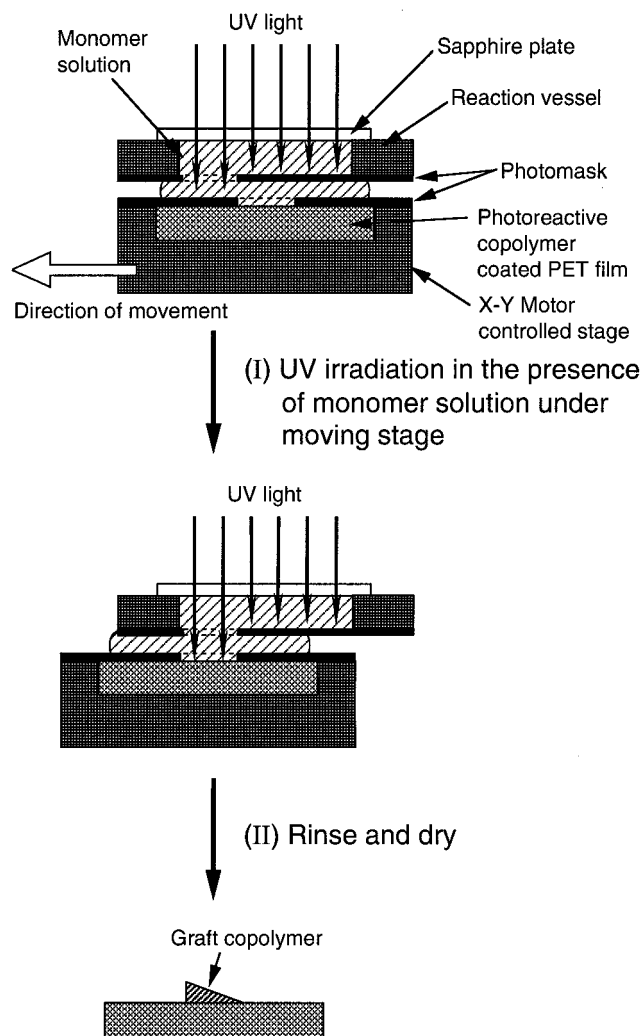


**Figure 6.** Schematic diagram of the preparation of a gradient surface varying unidirectionally in thickness of the photograft-copolymerized layer by using the combination of two types of photomasks and the X–Y step motor-controlled stage.

whereas the topographic roughness of the layer increased with the irradiation time (Figure 7: 2A and 2B). After about 14 min of UV irradiation (at position e), the measured thickness was approximately 1.5  $\mu\text{m}$ . The thickness of the grafted layer increased with irradiation time, indicating that the graft polymer layer thickness gradually increased with increasing distance from the nonirradiated end of the film. Other AFM studies revealed that thickness gradient surfaces were prepared by the surface photograft copolymerization of other monomers such as DMAPAAmMeI and MANa in a similar manner as described above (data not shown). Thus, the surface photograft copolymerization enabled a considerable degree of control of the thickness of graft-copolymerized layers.

*Cellular Response on Graft-Thickness Gradient Surface.* The cellular behavior on these gradient surfaces was examined. Figure 8 shows a phase-contrast photomicrograph montages of EC proliferation on these gradient surfaces at 3 days incubation. (The thickness of the grafted layers decreases from left to right.) The cell densities at the four domains (500  $\mu\text{m}$  length  $\times$  450  $\mu\text{m}$  width) of each gradient surface region were thoroughly examined. Figure 9 shows the cell density (500  $\mu\text{m}$   $\times$  450  $\mu\text{m}$ : 0.225  $\text{mm}^2$ ) as a function of distance from the photomask edge. On the polyDMAAm film strip, very few ECs were observed on the entire graft region, regardless of graft thickness. On

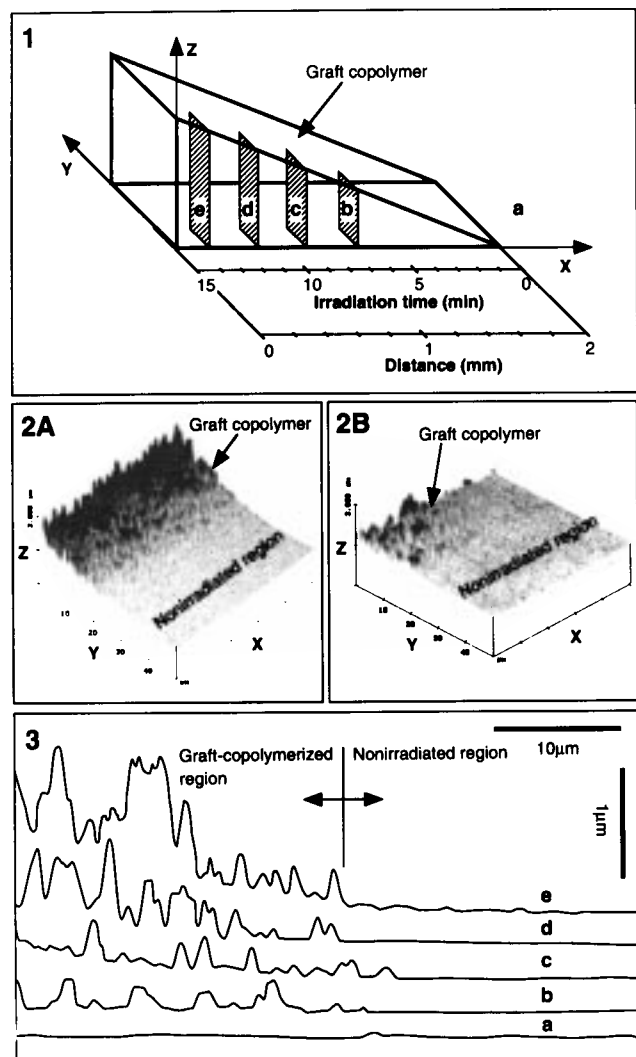


**Figure 7.** AFM sampling locations of the grafted region (1) and surface topological features of photograft-copolymerized surfaces as observed by AFM (2). AFM images of the gradient surface regions at  $200\ \mu\text{m}$  (position e in 1) (2A) and  $1100\ \mu\text{m}$  (position b in 1) (2B), which correspond to irradiation times of 13.5 and 6.75 min, respectively. Line scan spectra for selected regions corresponding to those in part 1 of the gradient film show the measured film thickness (3).

the polyDMAAmMeI film, some dependence on film thickness (chain length) was observed, where the total number of adhering ECs in the first three fields of 0–1.5 mm distance (Note that the edge of the photomask was defined as the distance “zero”) was significantly less than that in the last field (distance: 1.5–2.0 mm). The polyMANa film exhibited the greatest dependence on film thickness, with the total number of adhering ECs significantly increasing with increasing distance. Note that the rank order of the total number of adhering ECs in both the micropatterned and gradient film incubations is consistent, demonstrating the reproducibility of the EC response on these films.

### Discussion

In general, cellular responses such as adhesion, spreading, and proliferation on material surfaces, which are dependent on surface characteristics such as chemical composition and properties, have been studied on individual samples, which can be time-consuming and labor-

intensive.<sup>1–4,20–28</sup> In addition, an experimental error due to a slight difference in cell culture conditions may create false results. A substrate with a patterned surface gives the investigator the ability to expose an identical cell population under the same environmental conditions to a material with numerous spatially resolved surface chemistries.

Patterned surfaces have been prepared using a number of different techniques involving silane chemistry,<sup>29–32</sup> photolithography,<sup>33–38</sup> self assembly of alkane thiolates,<sup>39–41</sup> and glow discharge.<sup>42</sup> Of these techniques, photolithography has yielded photografted and derivatized surfaces with the greatest spatial resolution. In addition, unlike the method employed in this study, almost all of these techniques can only produce a modified surface with two different functionalized regions. While the method of sequential self-organization of alkanethiolates on a gold substrate has been demonstrated to produce multifunctionalized surfaces with similar regional specificity and precision, the use of a gold substrate limits its cost effectiveness and introduces potential immunogenic problems in gold allergic patients.<sup>39</sup> Additionally, the photograft copolymerization method used in this study can control graft chain length, and therefore the thickness of the graft polymer layer, by varying both the duration of photoirradiation and the photointensity of the UV light source. In this study, we were able to extend our previous work<sup>18</sup> to produce a modified surface with five different water soluble polymers regionally grafted with three-dimensional precision.

Surfaces where the proportion of functionalized groups relative to underlying substrate increases unidirectionally have been prepared to evaluate the effects of surface composition on protein adsorption and cellular behavior.<sup>5–12</sup>

(20) Lackie, J. M. *Cell Movement and Cell Behaviors*, Allen & Unwin: London, 1986.

(21) van Wachem, P. B.; Hogt, A. H.; Beugeling, T.; Feijen, J.; Bantjes, A.; Detmers, J. P.; van Aken, W. G. *Biomaterials* **1987**, *8*, 323.

(22) Bruil, A.; Terlingen, J. G.; Beugeling, T.; van Aken, W. G.; Feijen, J. *Biomaterials* **1992**, *13*, 915.

(23) Harkes, G.; Feijen, J.; Dankert, J. *Biomaterials* **1991**, *12*, 853.

(24) Goldberg, S.; Doyle, R. J.; Rosenberg, M. *J. Bacteriol.* **1990**, *172*, 5650.

(25) Watts, K. C.; Husain, O. *J. Clin. Pathol.* **1984**, *37*, 829.

(26) van Wachem, P. B.; Beugeling, T.; Feijen, J.; Bantjes, A.; Detmers, J. P.; van Aken, W. G. *Biomaterials* **1985**, *6*, 403.

(27) Horbett, T. A.; Waldburger, J. J.; Ratner, B. D.; Hoffman, A. S. *J. Biomed. Mater. Res.* **1988**, *22*, 384.

(28) Ratner, B. D.; Horbett, T.; Hoffman, A. S.; Hauschka, S. D. *J. Biomed. Mater. Res.* **1975**, *9*, 407.

(29) Healy, K. E.; Thomas, C. H.; Reznia, A.; Kim, J. E.; Mckeown, P. J.; Lom, B.; Hockberger, P. E. *Biomaterials* **1996**, *17*, 95.

(30) Britland, S.; Clark, P.; Connolly, P.; Moores, G. *Exp. Cell Res.* **1992**, *198*, 124.

(31) Kleinfeld, D.; Kahler, K. H.; Hockberger, P. E. *J. Neurosci.* **1988**, *8*, 4098.

(32) Lom, B.; Healy, K. E.; Hockberger, P. E. *J. Neurosci. Methods* **1993**, *50*, 385.

(33) Sugawara, T.; Matsuda, T. *J. Biomed. Mater. Res.* **1995**, *29*, 1047.

(34) Bhatia, S. N.; Tarmush, M. L.; Toner, M. *J. Biomed. Mater. Res.* **1997**, *34*, 189.

(35) Britland, S.; Clark, P.; Connolly, P.; Moores, G. *Exp. Cell Res.* **1992**, *198*, 124.

(36) Tarlov, M. J.; Burgess, D. R. F., Jr.; Gillen, G. *J. Am. Chem. Soc.* **1993**, *115*, 5305.

(37) Soekarno, A.; Lom, B.; Hockberger, P. E. *Neuroimage* **1993**, *1*, 129.

(38) Matsuda, T.; Sugawara, T. *J. Biomed. Mater. Res.* **1996**, *32*, 165.

(39) Lopez, G. P.; Albers, M. W.; Schreiber, S. L.; Carroll, R.; Peratta, E.; Whitesides, G. M. *J. Am. Chem. Soc.* **1993**, *115*, 5877.

(40) Tarlov, M. J.; Burgess, D. R. F., Jr.; Gillen, G. *J. Am. Chem. Soc.* **1993**, *115*, 5305.

(41) Sihghvi, R.; Kumar, A.; Lopez, G. P.; Stephanopoulos, G. N.; Wang, D. I. C.; Whitesides, G. M.; Ingber, D. E. *Science* **1994**, *264*, 696.

(42) Ranieri, J. P.; Bellamkonda, R.; Jacob, J.; Vargo, T. G.; Gardella, J. A.; Aebischer, P. *J. Biomed. Mater. Res.* **1993**, *27*, 917.

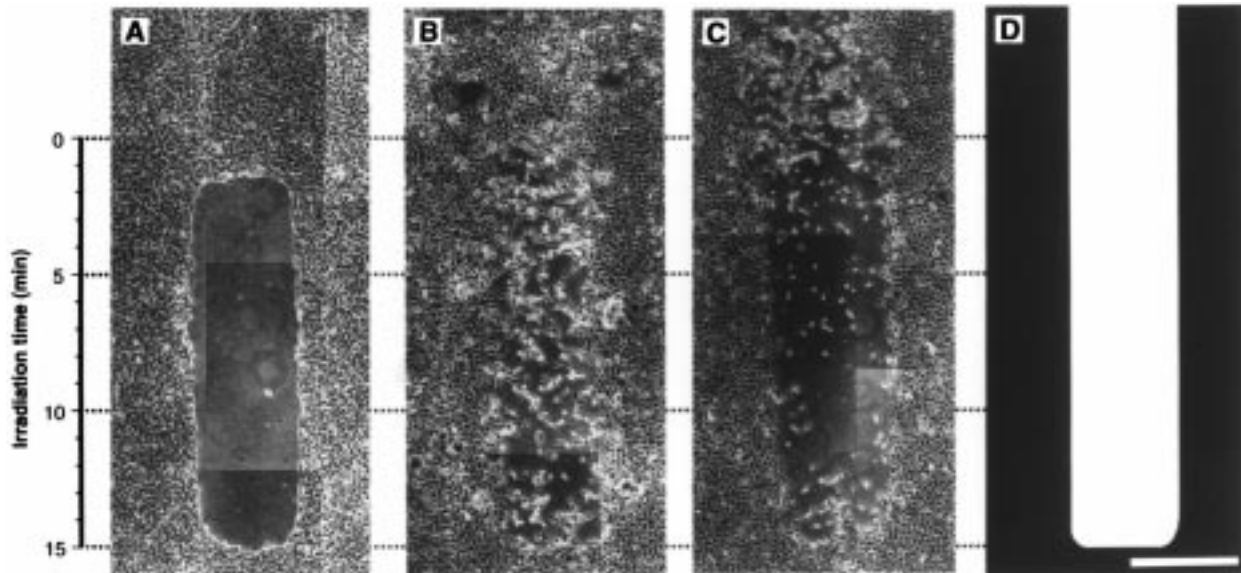


**Figure 8.** Phase-contrast micrographs ( $\times 200$ ) of bovine ECs' adhesion at 3 days after seeding on thickness gradient surfaces prepared by graft copolymerization with PDMAAm (A), PDMAPAAMeI (B), and PMANa (C). The photomask used in this experiment at the magnification corresponding to the microscopic images (D). Scale bar:  $300 \mu\text{m}$ .

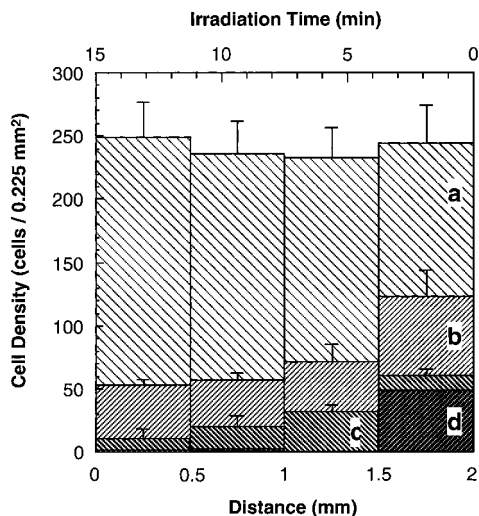


**Figure 9.** Cell density versus distance histogram at 3 days after incubation on a nongrafted photoreactive copolymer surface (a) and graft-polymer-layer-thickness gradient surfaces of PDMAPAAMeI (b), PMANa (c), and PDMAAm (d). The number of cells per unit area ( $0.225 \text{ mm}^2$ ) is plotted against the unit distance ( $500 \mu\text{m}$ ) from the edge of the photomask.

These chemical gradient surfaces have been prepared using several approaches, including using methylated silane-coupling reagents to convert hydroxyl groups to methyl groups on glass surfaces,<sup>8,9</sup> exposure of polymer surfaces to either radiofrequency plasma<sup>10</sup> or corona discharge<sup>11,12</sup> of increasing power unidirectionally to produce increasing densities of oxygen-containing functional groups, and the slow continuous immersion of poly(vinylene carbonate) film into an aqueous solution of sodium hydroxide.<sup>12</sup> Cellular adhesion studies on these surfaces uniformly demonstrated that increases in surface wettability corresponding to increases in the density of hydrophilic functional groups resulted in decreases in cellular adhesion. However, in addition to surface composition, graft chain length has been shown to be another important parameter determining cellular adhesion, thought to reflect the degree of surface hydration. To date, studies have been conducted on separate substrates prepared with polymer chains of different molecular

weights.<sup>43–45</sup> The technique involving copolymerization of dithiocarbamate with a sliding photomask and a motor-driven sample stage introduced in our previous study<sup>18</sup> has been extended to the successful preparation of three different thickness gradient surfaces, representing the first studies in which the effect of graft chain length upon cellular adhesion and proliferation has been directly studied on single samples.

The responses of cells on the aforementioned surfaces, particularly those relating to effects on cell morphology, function, migration, and proliferation, have been extensively studied.<sup>29–38,46–48</sup> Two distinctly different mechanisms participating in the cellular adhesion, which were studied on individual surfaces, have been discussed.<sup>1–4,20–28</sup> One is biospecific interaction of cellular membrane receptors and adsorbed adhesive proteins, typified by fibronectin.<sup>49–51</sup> Such surfaces, in which adsorption of the adhesive proteins present in a serum-containing medium preferentially occurs, are relatively hydrophobic or polar. The other mechanism proceeds via direct interaction of a negatively charged cellular membrane and cationically charged surfaces via electrostatic interactions. For example, surface coating of poly(L-lysine) or cationic synthetic polymers enhanced cellular adhesion.<sup>21–25</sup> The surfaces with the least protein adsorption and the easiest desorption have been identified as nonionic swellable surfaces. In fact, poly(ethylene glycol) (PEG)-derivatized surfaces reduced protein adsorption, and concomitantly, significantly reduced attachment of platelets and endothelial cells was noticed.<sup>52,53</sup>

In this study, on the regionally grafted surfaces, nonionic polyDMAAm- and polyHEMA-grafted surfaces inhibited

(43) Desai, N. P.; Hubbell, J. A. *J. Biomed. Mater. Res.* **1991**, *25*, 829.

(44) Bergstrom, K.; Osterberg, E.; Holmberg, K.; Hoffman, A. S.; Schuman, T.; Kozlowski, A.; Harris, J. H. *J. Biomater. Sci., Polym. Ed.* **1994**, *6*, 123.

(45) Matsuda, T.; Ito, S. *Biomaterials* **1994**, *15*, 417.

(46) Folkman, J.; Moscona, A. *Nature* **1978**, *273*, 345.

(47) Chen, C. S.; Mrksich, M.; Huang, S.; Whitesides, G. M.; Ingber, D. E. *Science* **1997**, *276*, 1425.

(48) Opas, M. *Dev. Biol.* **1989**, *131*, 281.

(49) Yamada, K. M.; Yamada, S. S.; Pastan, I. *Proc. Natl. Acad. Sci. U.S.A.* **1976**, *73*, 1217.

(50) Plerschbacher, M. D.; Ruoslahti, E. *Nature* **1984**, *309*, 30.

(51) Hynes, R. O. *Cells* **1992**, *69*, 11.



cell adhesion. Positively charged grafted chains, regardless of the type of cationic group (tertiary or quaternary amine), enhanced cell adhesion and growth, resulting in two-dimensional tissue formation. These observations are well-correlated with data in previous studies reported from many institutions.<sup>1-4,21-28</sup> The two negatively charged grafted chains, polyMANa and polySMAK, still generally promoted cell adhesion, but while the carboxylated polyMANa promoted cell proliferation, the sulfonated polySMAK markedly reduced cell adhesion and proliferation with increasing time of incubation (Figures 4 and 5). As for the participation of the sulfonate group in cellular adhesion, recent studies have shown that incorporation of a sulfonate group into segmented polyurethane significantly enhanced platelet adhesion in the particular medium, which was albumine-containing Tyrode's buffer.<sup>54</sup> It was discussed that platelets may have a binding site that is specific to sulfonate groups. On the other hand, sulfonated, segmented polyurethanes significantly reduced platelet adhesion in whole blood or plasma media,<sup>55,56</sup> which was speculated due to fibrinogen and thrombin interactions with the sulfonated polymer surface.<sup>54</sup> These interactions are believed to interfere with fibrin formation and to result in heparin-like catalysis of the inhibition of thrombin by ATIII.<sup>57</sup> Similarly, sulfonate group-bearing PEG-grafted surfaces significantly reduced platelet adhesion.<sup>53</sup> The proposed mechanism is due to synergistic actions of high water uptake derived from the strongly negatively charged group and high chain mobility derived from the PEG segment. We speculate that the very strong hydration power of the sulfonate group with chain reorganization may explain this time dependent phenomenon. That is, the weak adhesion interaction of adhered cells with polySMAK results in markedly reduced cell spreading, which appears to induce cell detachment with time. Anchorage-dependent cells such as ECs require good-spreading for cell proliferation. Otherwise, apoptosis of the cells eventually occurs on such a surface.<sup>47</sup> Cytotoxicity of the polySMAK is also possible, although there are no previous studies which demonstrate sulfonate groups are particularly harmful to cells. Clearly, each of these different grafted regions elicited its own cellular response, suggesting that this photograft copolymerization method can be easily utilized to modify surfaces to maximize beneficial cell-device interactions.

On the gradient thickness surfaces, regions grafted with longer chain lengths corresponding to thicker graft layers showed significantly reduced cell adhesion,<sup>5-12</sup> consistent with previous studies describing markedly decreased

adhesion on grafted or hydrogel surfaces with swellable or hydrated polymer chains.<sup>43,44,58-61</sup> However, unlike the polyDMAAmMeI and polyMANa gradient thickness surfaces, which showed moderate decreases in cell adhesion with increasing graft thickness, polyDMAAm grafts less than a critical thickness sustained monolayer growth of endothelial cells, suggesting that there exists a threshold graft chain length for nonadhesion of endothelial cells (Figures 4 and 9). The differences in cellular behaviors observed on these gradient thickness surfaces suggest that graft chain length is an unexploited tool to be used for device design. Similar studies with gradient thickness nonswellable surfaces may provide insight on the interactions which were observed in this study. Although all grafted surfaces in this study were water soluble, nonswellable surfaces, both polar and nonpolar, can easily be prepared using this method.

In summary, a self-perpetuating photograft copolymerization method based on the photochemistry of an iniferter benzyl *N,N*-diethyldithiocarbamate has been used in combination with an X-Y controlled step motor to achieve three-dimensional regional and chemically specific micron level precision-patterned surfaces. Substrates with patterned surfaces offer opportunities to study an identical cell population on a material with either numerous spatially resolved surface chemistries or varying polymer graft chain lengths under the same environmental conditions. This technique also affords unprecedented control over device design, making it possible to complete on one device surface modifications necessary for multiple microenvironments encountered at different device-cell interfaces. Moreover, its experimental simplicity makes automation feasible. In fact, a new laboratory scale mass production apparatus has been developed that employs a UV light transmitted through a quartz optical fiber with sample movement controlled via computer-assisted design (CAD), enabling automated multiple sample preparation. This will be reported in the near future.

**Acknowledgment.** The authors would like to acknowledge support provided for J.H. by the Summer Institute in Japan Program, which is jointly supported by the Science and Technology Agency of Japan, the U.S. National Science Foundation, the U.S. National Institutes of Health, and the U.S. Agricultural Research Service. This study was financially supported by the Promotion of Fundamental Studies in Health Science of the Organization for Pharmaceutical Safety and Research (OPSR) under Grant No. 97-15.

LA9810511

(52) Lopez, G. P.; Ratner, B. D.; Tidwell, C. D.; Haycox, C. L.; Rapoza, R. J.; Horbett, T. A. *J. Biomed. Mater. Res.* **1992**, *26*, 415.

(53) Han, D. K.; Park, K. D.; Kim, Y. H. *J. Biomater. Sci., Polym. Ed.* **1988**, *9*, 163.

(54) Skarja, G. A.; Brash, J. L. *J. Biomed. Mater. Res.* **1997**, *15*, 439.

(55) Grasel, T. G.; Cooper, S. L. *J. Biomed. Mater. Res.* **1997**, *15*, 439.

(56) Okkema, A. Z.; Visser, S. A.; Cooper, S. L. *J. Biomed. Mater. Res.* **1991**, *25*, 1371.

(57) Silver, J. H.; Hart, A. P.; Willaims, S. L.; Cooper, S. L.; Charef, S.; Labarre, D.; Jozefowicz, M. *Biomaterials* **1992**, *13*, 339.

(58) Fujimoto, K.; Inoue, H.; Ikada, Y. *J. Biomed. Mater. Res.* **1993**, *27*, 1559.

(59) Ikada, Y.; Suzuki, M.; Taniguchi, M.; Iwata, H.; Taki, W.; Miyake, H.; Handa, H. *Radiat. Phys. Chem.* **1981**, *18*, 1207.

(60) Matsuda, T.; Sugawara, T. *J. Biomed. Mater. Res.* **1995**, *29*, 749.

(61) Nakayama, Y.; Matsuda, T. *J. Polym. Sci., Polym. Chem. Ed.* **1993**, *31*, 977.